# Exotic Kondo Effect from Magnetic Trimers

B. Lazarovits,[1] P. Simon,[2] G. Zaránd,[3] and L. Szunyogh[1,3]

[1]*Center for Computational Materials Science, Vienna University of Technology, A-1060, Gumpendorferstr. 1.a., Vienna, Austria*
[2]*Laboratoire de Physique et Modélisation des Milieux Condensés, CNRS et Université Joseph Fourier, 38042 Grenoble, France*
[3]*Theoretical Physics Department, Budapest University of Technology and Economics, Budafoki út 8. H-1521 Hungary*
(Received 15 July 2004; published 9 August 2005)

Motivated by the recent experiments of Jamneala *et al.* [Phys. Rev. Lett. **87**, 256804 (2001)] by combining *ab initio* and renormalization group methods, we study the strongly correlated state of a Cr trimer deposited on gold. Internal orbital fluctuations of the trimer lead to a huge increase of $T_K$ compared to the single ion Kondo temperature explaining the experimental observation of a zero-bias anomaly for the trimers. The strongly correlated state seems to belong to a new yet hardly explored class of non-Fermi-liquid fixed points.

In recent years, atomic scale resolution scanning tunneling microscopy (STM) proved to be a spectacular tool to probe the local density of states around Kondo impurities adsorbed on a metallic surface [1,2]. Experiments were performed with single Ce atoms on Ag [1], and Co atoms on Au [2] and Cu surfaces [3,4]. When the STM tip is placed directly on the top of the magnetic adatom, a sharp resonance appears in the differential conductance at low bias and disappears when the STM tip is moved away from the impurity or when the substrate temperature is raised above the Kondo temperature $T_K$. This zero bias anomaly appears as the main signature of the Kondo effect and results from the screening of the adatom spin by the surrounding (bulk and surface) conduction electrons. The precise line shape of the resonance can well be understood in terms of a Fano resonance, an interference phenomenon occurring because of two possible tunneling channels: a direct channel between the tip and the impurity and a second channel between the tip and the surface [2,5–7].

The manipulation of single atoms on top of a surface with an STM tip has also been proven useful to build clusters of atoms with well-controlled interatomic distances. For example, Manoharan *et al.* [3] manufactured an elliptical quantum corral of Co adatoms and found that, when an extra Co adatom is placed at one focus of the elliptical corral, a "mirage" of the Kondo resonance can also be observed at the other focus. Another intriguing result was found recently for Cr trimers on a gold surface by Jamneala *et al.* [8]. Whereas isolated Cr monomers or dimers display featureless signals in STM spectra at $T = 7$ K, Cr trimers exhibit two distinct electronic states depending on the atomic positions: a sharp Kondo resonance of width $T_K \sim 50$ K was found for an equilateral triangle, while the STM signal of an isosceles triangle did not show any particular feature. Furthermore, the Cr trimers were reversibly switched from one state to another. As schematically depicted in Fig. 1, Cr atoms forming an equilateral triangle are expected to occupy nearest neighbor sites on the gold surface [Au(111)], allowing therefore geometric frustration [8]. Such a compact magnetic nanocluster is of

very much theoretical interest due to the interplay between Kondo physics and magnetic frustration that may generate internal orbital fluctuations. This system can indeed be regarded as the smallest and simplest frustrated Kondo lattice and, as we will see, embodies a very rich behavior. We show in this Letter that internal orbital fluctuations in the Cr equilateral trimer lead to a huge increase of the Kondo temperature in agreement with the experiment and we argue that the low-energy physics of the system is governed by a new non-Fermi-liquid fixed point [9].

In this Letter we shall present a careful study of the strongly correlated state of the Cr trimer depicted in Fig. 1. In order to construct an effective Hamiltonian for this system, we first performed *ab initio* calculations [10] to study the electronic structure of the Cr ions forming the cluster, and verified that the Cr ions are within a very good approximation in $d^5$ spin $S_{Cr} = \tilde{S} = 5/2$ states, and display relatively small valence fluctuations. Under these conditions, the Hamiltonian describing the nanocluster can well be approximated as

$$H = H_{\text{spin}} + \frac{G}{2} \sum_{i,\sigma,\sigma'} \vec{S}_i \psi_{i\sigma}^\dagger \vec{\sigma}_{\sigma\sigma'} \psi_{i\sigma'}, \qquad (1)$$

where $H_{\text{spin}}$ describes the interaction between the Cr spins
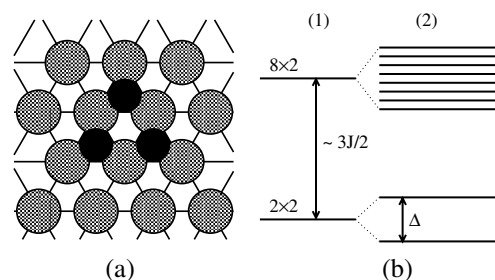


FIG. 1. (a) Top view of the equilateral Cr cluster on the Au(111) surface. Au and Cr atoms are indicated by gray and black circles, respectively. (b) Eigenstate structure of $H_{\text{spin}}$ of the Cr cluster (1) in the absence and (2) in the presence of spin-orbit coupling.

$\vec{S}_i$ at sites $i = 1, \ldots, 3$, and $G$ denotes the Kondo coupling between each Cr spin and the conduction electrons in the substrate. Note that Eq. (1) incorporates only the exchange generated by the most strongly hybridizing $d$ state. This approximation is justified by the observation that the Kondo effect is exponentially sensitive to the strength of hybridization, and therefore hybridization with other $d$ states is not expected to change our results. Correspondingly, it is sufficient to consider only the hybridization with a single conduction electron state, $\psi_i$, leading to Eq. (1). Note, however, that these states may overlap with each other and in general $\{\psi_i, \psi_j^\dagger\} \neq \delta_{i,j}$. As we demonstrate later by *ab initio* calculations, the effective spin-spin interaction $H_{\text{spin}}$ in Eq. (1) is rather well approximated by a dipolar term $H_{\text{spin}} \approx H_{\text{dipol}} = J\Sigma_{(i,j)}\vec{S}_i\vec{S}_j$, where the coupling $J \approx 1600$ K turns out to be antiferromagnetic.

Since the Kondo temperature $T_K \sim 50$ K generated by $G$ is expected to be much smaller than the exchange coupling $J$, and we only wish to describe the physical behavior of the cluster around the low-energy scale $\sim T_K$, we shall first diagonalize $H_{\text{spin}}$ and construct an effective Hamiltonian to describe quantum fluctuations of the cluster spins. The low-energy section of the spectrum of $H_{\text{dipol}}$ is sketched in Fig. 1(b): there are *two* different ways to construct states with total spin $S = 1/2$ that minimize $H_{\text{dipol}}$. As a consequence, the ground state is fourfold degenerate, the extra degeneracy being associated with a two-dimensional representation of the $C_{3v}$ symmetry of the cluster. These four spin states can thus be labeled as $|\sigma, \mu\rangle$, where $\sigma = \uparrow, \downarrow$ denotes the spin and $\mu = \pm$ is a chiral index: $C_3|\sigma, \mu\rangle = e^{i\mu 2\pi/3}|\sigma, \mu\rangle$. Note that the four states remain degenerate as long as $H_{\text{spin}}$ is SU(2) invariant, and only spin-orbit coupling related effects discussed later can split their degeneracy.

To obtain the effective Hamiltonian $H_{\text{eff}}$ within the subspace $\{|\sigma, \mu\rangle\}$, we first construct the states $|\sigma, \mu\rangle$ explicitly using Clebsch-Gordan coefficients and then evaluate the matrix elements of the Kondo exchange, $H_K \equiv \frac{G}{2}\Sigma_{i,\sigma,\sigma'}\vec{S}_i\psi_{i\sigma}^\dagger\vec{\sigma}_{\sigma\sigma'}\psi_{i\sigma'}$ within this subspace. The effect of virtual transitions into the high energy subspace on the effective low-energy couplings is neglected assuming $G/J \ll 1$. It is convenient to introduce the following Fermionic fields, $\psi_{\sigma\mu} \equiv \frac{1}{\sqrt{3}}\Sigma_j e^{i\mu j2\pi/3}\psi_{j\sigma}$, where now $\mu$ takes three possible values, $\mu = 0, \pm$. After tedious algebra the effective Hamiltonian takes a rather simple form in this notation,

$$H_{\text{eff}} = \frac{G}{6}[\vec{S}\psi^\dagger\vec{\sigma}\psi - (2\tilde{S} + 1)(\vec{S}T^+\psi^\dagger\vec{\sigma}\tau^-\psi + \text{H.c.})], \quad (2)$$

where $\vec{S}$ denotes a spin 1/2 operator acting on the spin indices of $|\sigma, \mu\rangle$, and the orbital pseudospin operators $T^\pm$ are standard operators raising/lowering the chiral spin $\mu$. The operators $\tau^\pm$ in Eq. (2) change the angular quasimomentum of the conduction electrons by one unit, $\tau^\pm_{\mu,\mu'} = \delta^{(3)}_{\mu,\mu'\pm1}$, where $\delta^{(3)}$ denotes the Kronecker delta function

modulo 3. Note that $H_{\text{eff}}$ depends on the magnitude of the initial local spins enhancing the second term by a factor $2\tilde{S} + 1$.

To determine the low-energy dynamics of the system and the Kondo scale $T_K$, we carried out a perturbative renormalization group (RG) analysis of the system. Within the RG, high energy conduction electrons are integrated out and the original bandwidth $D_0$ is gradually reduced to smaller and smaller values $D$. Two stages must be distinguished in the course of the RG procedure: (a) for $D \gg J$ the neighboring Cr spins behave as *independent* spins. (b) For $D \ll J$, on the other hand, the Cr spins are tied together by their exchange interaction, and the effective Hamiltonian (2) can be used. In the first regime only $G$ is renormalized according to the usual scaling equation [11]:

$$\frac{dG}{dl} = \varrho_0 G^2 - \frac{1}{2}\varrho_0^2 G^3 \qquad (D \gg J), \qquad (3)$$

where $l = \ln(D_0/D)$ is the scaling parameter and $\varrho_0$ denotes the local density of states and is related to the propagator of the field $\psi_{\sigma j}$ through $\langle\psi_{\sigma j}(t)\psi_{\sigma j}^\dagger(0)\rangle \approx -i\varrho_0/t$.

At energies (time scales) below $J$, we can thus use the effective Hamiltonian (2), but with a conduction electron cutoff reduced to $D = \tilde{D}_0 \sim 3J/2$ and the coupling $G$ replaced by an effective coupling $G \to \tilde{G} \equiv G(l = \ln(D_0/\tilde{D}_0))$. In this regime, however, the RG analysis becomes more complicated, and additional terms are generated in the Hamiltonian. To allow for the generation of these terms we first introduce a very general Hamiltonian of the form:

$$H \equiv \sum_{\alpha,\beta=1,\ldots,4} \sum_{p,q=1,\ldots6} |\alpha\rangle\langle\beta|\psi_p^\dagger V_{pq}^{\alpha\beta}\psi_q, \qquad (4)$$

where $\alpha, \beta = \{\sigma = \pm, \mu = \pm\}$ and $p, q = \{\sigma = \pm, \mu = \pm, 0\}$ denote composite indices referring to the ground state multiplet and the conduction electrons, respectively. To obtain $T_K$ we solved numerically the RG equations derived in Ref. [12] for this general model. The initial values of the couplings $V_{pq}^{\alpha\beta}$ can easily be determined from Eq. (2) at $D = \tilde{D}_0$. However, special care is needed to define the dimensionless couplings entering the scaling equations: since $\{\psi_i, \psi_j^\dagger\} \neq \delta_{i,j}$, the off-diagonal-correlation function decays in general as $\langle\psi_{\sigma1}(t)\psi_{\sigma2}^\dagger(0)\rangle \approx -i\alpha\varrho_0/t$, with an overlap parameter $\alpha < 1$. As a result, the density of states in the electronic channels depends on the chiral index: $\varrho_\mu = \varrho_0(1 + 2\alpha)$ for $\mu = 0$ and $\varrho_\mu = \varrho_0(1 - \alpha)$ for $\mu = \pm$. These densities of states enter the dimensionless couplings of Ref. [12] as $v_{pq}^{\alpha\beta} \equiv \sqrt{\varrho_p\varrho_q}V_{pq}^{\alpha\beta}$. The parameter $\alpha$ can be estimated using a free electron model [13], but a simple tight binding model can also be used to estimate it [14] and is typically in the range $0.2 < \alpha < 0.6$.

The advantage of the RG method discussed above is that it sums up systematically leading and subleading logarith-

mic corrections and provides an unbiased tool to obtain $T_K$, even without knowing the structure of the fixed point Hamiltonian. This is in sharp contrast with a variational study as the one developed by Kudasov and Uzdin for this problem [15], which only gives an upper bound on $T_K$, gets even the exponent of Kondo temperature incorrectly (see, e.g., in Ref. [11]), and the result of which depends essentially on the specific variational ansatz made. Furthermore, the perturbative renormalization group enables one to gain some insight into the structure and symmetry of the fixed point Hamiltonian describing the physics of Eq. (1) below the Kondo scale.

The Kondo temperature can be defined as the energy scale at which the norm of the effective couplings, $N \equiv (\Sigma_{\alpha,\beta,p,q}|v_{pq}^{\alpha\beta}|^2)^{1/2}$ reaches the strong coupling limit $[N(D = T_K) \equiv 0.7]$. For $\alpha = 1$ only the field $\psi_{\mu=0}$ couples to the cluster, and the scaling equations reduce to those of an isolated Cr spin. Therefore, in this limit $T_K$ is the same as that of an isolated Cr ion, $T_K^{(0)}$. In the inset of Fig. 2 we show the Kondo temperature of the trimer as a function of the Kondo temperature of a single Cr ion for two typical values of the overlap parameter $\alpha$ and for an intermediate cutoff $\tilde{D}_0 = 5000$ K $\sim 3J$. The trimer's Kondo temperature is orders of magnitude larger than that of the single Cr ion, and for $0.001$ K $< T_K^{(0)} < 0.1$ K (which is in agreement with the small bulk Kondo temperature of Cr in Au [16]), yields a trimer Kondo scale $10$ K $< T_K < 100$ K. We also find that $T_K \approx C(\alpha)\sqrt{\tilde{D}_0 T_K^{(0)}}$, with $C(\alpha)$ a constant of the order of unity. This increase is clearly due to the presence of orbital fluctuations and gives a natural explanation to the fact that the Kondo effect has not been observed experimentally for a single Cr ion on Au [8]. Note, however, that this increase is peculiar to the case of large cluster spins $\tilde{S}$, and no such a dramatic increase appears for spin $\tilde{S} = 1/2$ trimers, in contrast to the results
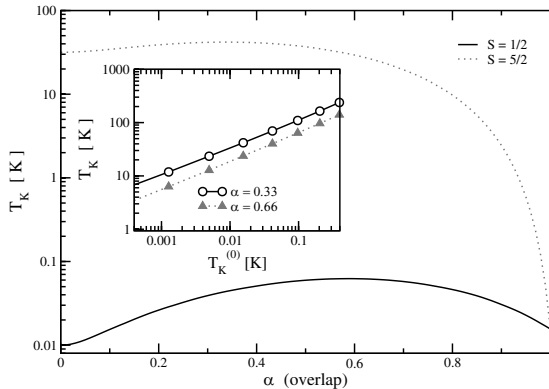


FIG. 2.  Kondo temperature as a function of the overlap parameter $\alpha$ for a cluster formed of atoms with spin $\tilde{S} = 5/2$ and spin $\tilde{S} = 1/2$. We used $\tilde{D}_0 = 5000$ K $\approx 3J$ and a dimensionless coupling $G = 0.09$. The inset shows in a log-log plot the Kondo temperature of the trimer as a function of the single Cr's Kondo temperature for two overlap parameters $\alpha = 0.33$ and $\alpha = 0.6$.

of Ref. [15]. This important difference of behavior between $\tilde{S} = 1/2$ and $\tilde{S} = 5/2$ is highlighted in Fig. 2, where on a log scale we displayed $T_K$ as a function of the overlap parameter for the specific choice, $G = 0.09$, corresponding to a trimer Kondo scale $\sim 40$ K and $T_K^{(0)} \approx 0.01$ K.

Distorting the equilateral trimer configuration, we clearly lift the fourfold ground state degeneracy of $H_{\text{spin}}$ and therefore suppress this Kondo cluster effect and no enhancement of the Kondo temperature is expected. Geometric distortion in our formalism appears in fact as a strong orbital magnetic field. This gives a natural explanation why the isosceles Cr trimer displayed no Kondo resonance at the experimental temperature $T = 7$ K.

The RG flows also allow us to gain information on the symmetry of the low-energy fixed point, governing the $T \rightarrow 0$ dynamics of the cluster, since dynamically generated symmetries typically show up already within the perturbative RG. Surprisingly enough, analyzing the structure and algebraic properties of the fixed point couplings $v_{pq}^{\alpha\beta}$, we find that it is *neither* the familiar SU(4) Fermi liquid fixed point [17] *nor* the two-channel Kondo fixed point [18]. We find instead that the fixed point Hamiltonian takes the following from:

$$H_{\text{fp}} = \alpha \vec{S}\,\vec{\sigma} + \beta \vec{S}\,\vec{\sigma}\,L_z^2 + \gamma T^z L^z$$
$$+ \delta \vec{S}\,\vec{\sigma}(T^- L^+ + T^+ L^-), \quad (5)$$

where for simplicity we suppressed the fermion fields. The operators $L^{\pm}$ and $L^z$ above denote standard $L = 1$ angular momentum matrices acting on the fermionic orbital spin. While this Hamiltonian clearly has an enlarged U(1) symmetry (replacing the original $C_3$ symmetry), it remains nevertheless anisotropic in orbital space. This structure allows us to identify this fixed point with the non-Fermi-liquid fixed point identified first in Ref. [9] using the numerical renormalization group method for the simpler problem of a spin $1/2$ model trimer. A supplementary strong coupling analysis can be used to support that this fixed point is indeed at finite couplings and must therefore be of non-Fermi-liquid character. We also find that this fixed point is unstable to general Hermitian perturbations (another indication of unstable fixed points), under which it flows to the familiar stable SU(4) Fermi liquid fixed point [17]. On the other hand, we could not find additional terms respecting SU(2) $\times C_{3v}$ symmetry that would render the strange fixed point unstable. The analysis of the physical properties of this non-Fermi-liquid fixed point is beyond the scope of the present Letter, but the thermodynamical, transport, and tunneling (STM) properties are expected to show anomalous scaling properties [9,19].

So far we fully neglected the effect of spin-orbit coupling. However, spin-orbit coupling removes the fourfold degeneracy of the ground state of $H_{\text{spin}}$, and splits it up into two Kramers doublets. To build a consistent picture (and also to have a non-Fermi-liquid regime) this splitting $\Delta$ must be smaller than $T_K$. In order to estimate the splitting
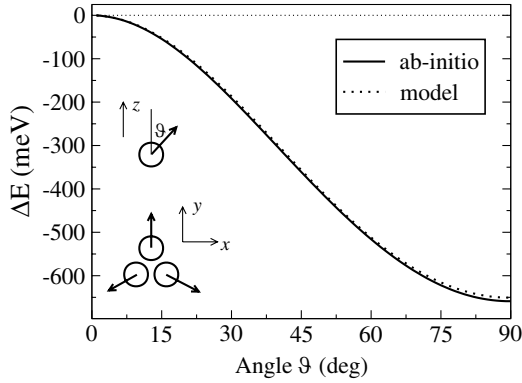
FIG. 3.   Energy of the Cr trimer as a function of the direction of magnetization computed using a relativistic *ab initio* method (full line) and the effective model, Eq. (6) (dotted line), for the particular configurations sketched in the inset. In this example only the angle $\vartheta$ with respect to the $z$ axis is varied (upper inset). The lower inset shows the projections of the magnetization onto the surface ($xy$ plane).

we performed relativistic *ab initio* calculations [10] by fixing the orientation of Cr spins, $\vec{S}_j \rightarrow S\vec{\Omega}_j$, and determined the energy of the cluster as a function of the spin orientations, $E[\{\vec{\Omega}_j\}]$ [14]. The energy of the cluster can excellently be approximated by the following expression,

$$E[\{\vec{\Omega}_j\}] = S^2 \sum_{i,j=1}^{3} \sum_{\alpha,\beta=x,y,z} J_{ij}^{\alpha\beta} \Omega_i^\alpha \Omega_j^\beta + H_Q. \quad (6)$$

The dominant term of the interaction turns out to be the simple SU(2) invariant exchange interaction studied in the first part of the Letter. The term $H_Q$ above contains SU(2) invariant quadrupolar couplings and three-spin interactions. While these turn out to be of the same order of magnitude as the anisotropy of the exchange interaction, $H_Q$ does not lead to a splitting of the ground state degeneracy in contrast to anisotropy terms. In Fig. 3 the *ab initio* values of the energy of the cluster are compared with energies of the effective Hamiltonian in Eq. (6) for a particular configuration of the Cr spins. Having determined the exchange couplings above, we performed first order perturbation theory within the degenerate subspace of the trimer to obtain $\Delta \approx 20$ K, which is indeed less than the experimentally observed Kondo temperature, $T_K \sim 50$ K. This splitting will ultimately destroy the non-Fermi-liquid properties predicted above; however, the energy scale $\Delta^*$ at which this happens is expected to be smaller than $\Delta$ similar to the two-channel Kondo model, where $\Delta^* \sim \Delta^2/T_K$.

For Cr on gold the ratio $T_K/\Delta^*$ is probably too small to observe the non-Fermi-liquid physics. However, it should be possible to observe it in other systems: Cr on Ag, e.g., is a promising candidate, since the lattice constant of Ag is about the same as that of Au (important to have antiferromagnetic coupling between magnetic ions), while the spin-orbit coupling is much weaker. Our calculations show that

in this case $\Delta \sim 1$ K, and a much wider non-Fermi-liquid range may be accessible. Similar structures could be constructed from single electron transistors. In this case the atoms would be replaced by quantum dots. The great advantage of such a device would be that (1) it would be highly tunable and (2) it would allow for *transport* measurements, though it is not easy to guarantee the perfect symmetry of the device.

[1] J. Li, W.-D. Schneider, R. Berndt, and B. Delley, Phys. Rev. Lett. **80**, 2893 (1998).
[2] V. Madhavan, W. Chen, T. Jamneala, M. F. Crommie, and N. S. Wingreen, Science **280**, 567 (1998); Phys. Rev. B **64**, 165412 (2001).
[3] H. C. Manoharan, C. P. Lutz, and D. M. Eigler, Nature (London) **403**, 512 (2000).
[4] N. Knorr, M. A. Schneider, L. Diekhoener, P. Wahl, and K. Kern, Phys. Rev. Lett. **88**, 096804 (2002).
[5] A. Schiller and S. Hershfield, Phys. Rev. B **61**, 9036 (2000).
[6] O. Újsághy, J. Kroha, L. Szunyogh, and A. Zawadowski, Phys. Rev. Lett. **85**, 2557 (2000).
[7] M. Plihal and J. W. Gadzuk, Phys. Rev. B **63**, 085404 (2001).
[8] T. Jamneala, V. Madhavan, and M. F. Crommie, Phys. Rev. Lett. **87**, 256804 (2001).
[9] B. C. Paul and K. Ingersent, cond-mat/9607190.
[10] B. Lazarovits, L. Szunyogh, and P. Weinberger, Phys. Rev. B **65**, 104441 (2002).
[11] A. C. Hewson, *The Kondo Problem to Heavy Fermions* (Cambridge University Press, Cambridge, England, 1993).
[12] G. Zaránd, Phys. Rev. Lett. **77**, 3609 (1996).
[13] V. L. Libero and L. N. Oliveira, Phys. Rev. Lett. **65**, 2042 (1990).
[14] B. Lazarovits *et al.* (to be published).
[15] Yu. B. Kudasov and V. M. Uzdin, Phys. Rev. Lett. **89**, 276802 (2002).
[16] C. Rizzuto, Rep. Prog. Phys. **37**, 147 (1974).
[17] L. Borda, G. Zaránd, W. Hofstetter, B. I. Halperin, and J. von Delft, Phys. Rev. Lett. **90**, 026602 (2003); G. Zaránd, A. Brataas, and D. Goldhaber-Gordon, Solid State Commun. **126**, 463 (2003); K. Le Hur and P. Simon, Phys. Rev. B **67**, 201308R (2003).
[18] N. Shah and A. J. Millis, Phys. Rev. Lett. **91**, 147204 (2003).
[19] K. Ingersent, A. W. W. Ludwig, and I. Affleck, cond-mat/0505303.